

Metallocarborane chemistry of the *hypho*-[6,7-C₂B₆H₁₃][−] anion: the formation of uniquely structured metallocarboranes [5-Cp^{*}-*arachno*-5, 4, 6-RhC₂B₆H₁₂] and [2, 5-Cp₂^{*}-10-Me-*nido*-2, 5, 1-Rh₂CB₆H₉] (Cp^{*} = η⁵-C₅Me₅[−]): complete rhodium analogues of *arachno*-4,6-C₂B₇H₁₃ and *nido*-1-CB₈H₁₂

Michael G.S. Londesborough ^{a,*}, Zbyněk Janoušek ^a, Bohumil Štíbr ^a, Ivana Čísařová ^b

^a Institute of Inorganic Chemistry, Academy of Sciences of the Czech Republic (Research Center for New Inorganic Compounds and Advanced Materials, University of Pardubice), 250 68, Řež, The Czech Republic

^b Department of Inorganic Chemistry, Faculty of Natural Science of Charles University, Albetov 2030, 128 40 Prague 2, Czech Republic

Received 14 January 2004; accepted 19 April 2004

Abstract

Reaction of the tetramethylammonium salt of the *hypho*-[6,7-C₂B₆H₁₃][−] anion (**1**) with the [Rh(η⁵-C₅Me₅)Cl₂]₂ dimer in THF solution, resulted in the formation of a novel nine-vertex metalladiborane [5-Cp^{*}-*arachno*-5,4,6-RhC₂B₆H₁₂] (**2**) (Cp^{*} = η⁵-C₅Me₅). An analogous reaction, but in the presence of PS (PS = ‘proton-sponge’ = 1,8-bis-(dimethylamino)-naphthalene), resulted in the bimetallic nine-vertex species [2, 5-Cp₂^{*}-10-Me-*nido*-2, 5, 1-Rh₂CB₆H₉] (**3**). Compounds **2** and **3** are structural analogues of carboranes *arachno*-4,6-C₂B₇H₁₃ (**4**) and *nido*-1-CB₈H₁₂ (**5**), respectively. The formation of compound **3** is associated with an extrusion of one of the cluster carbon atoms into an *exo*-polyhedral position and exhibits a very rare nine-vertex *nido* metallaborane structure with interesting features. Both species **2** and **3** were characterized by multinuclear NMR measurements and single-crystal X-ray diffraction studies.

© 2004 Elsevier B.V. All rights reserved.

Keywords: Boranes; Metallocarboranes; Rhodium complex; *Hypho*

1. Introduction

The geometries and electron-counts of the vast majority of known carborane species fall under the structural categories of *closo*, *nido* and *arachno* carboranes. The *hypho* structural series of parent carboranes, which consists of compounds with a 2*n* + 8 (where *n* is the number of polyhedral vertices) electron count is, as yet, solely represented by the [6,7-C₂B₆H₁₃][−] anion (**1**) (for new numbering see Scheme 1).

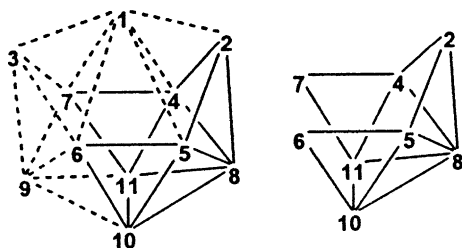
The synthesis of anion **1**, referred to as the “helmet anion” [**1**] due to its helmet-like appearance, was reported some years ago [**1,2**]. Since this discovery, however, little investigation into the reactive properties of **1** has been made. In this context, we present here the results from a part of an investigation into the reactivity of **1** by means of a description of two new metallocarborane compounds formed from its reaction with [Cp^{*}RhCl₂]₂.

2. Results and discussion

The [Cp^{*}RhCl₂]₂ dimer appears to be a valuable synthon in metallaborane chemistry, and has precedent in

* Corresponding author. Tel.: +420-266-173-109; fax: +420-220-940-161/941-502.

E-mail address: michael@iic.cas.cz (M.G.S. Londesborough).



Scheme 1. Derivation of an eight-vertex *hypho* structure, and its numbering, by the removal of three adjacent vertices from an 11-vertex *closo* shape.

its use for the insertion of rhodium centers into borane-cluster frameworks [3]. For this reason it was thought to be an appropriate candidate for metal–atom insertion and thus cage-expansion of the helmet anion; one of the initial targets from a series of exploratory reactions designed to evaluate the chemical versatility of the *hypho* anion **1**.

Thus, the reaction of the $[\text{NMe}_4]$ salt of **1** in THF with an equimolar equivalent of $[\text{Cp}^*\text{RhCl}_2]_2$ (see path [i] of Scheme 2) gave as a main product (22% yield) the new nine-vertex metallocarborane $[5\text{-Cp}^*\text{-}arachno\text{-}5,4,6\text{-RhC}_2\text{B}_6\text{H}_{12}]$ (**2**) and constitutes a polyhedral-expansion from eight to nine cluster vertices.

Compound **2** was structurally characterized using both multinuclear NMR spectroscopy and a single-crystal X-ray diffraction analysis. Fig. 1 is an illustration of the crystallographically determined structure of compound **2**. It has a typical nine-vertex *arachno* geometry that is common among other nine-vertex *arachno* borane and carborane species and is *isoelectronic* with, for example, $\text{K}[\text{B}_9\text{H}_{14}]$ [4] and $4,6\text{-C}_2\text{B}_7\text{H}_{13}$ (**4**) [5]. The crystallographic structure suggests that complex **2** is a straightforward structural analogue of the latter dicarbaborane with the $\{\text{Cp}^*\text{Rh(III)}^{2+}\}$ fragment replacing the *isobal* $\{\text{B(5)H}\}$ vertex.

A graphical comparison of the ^{11}B NMR spectra of compound **2** and carborane **4**, shown in Fig. 2 (bottom traces), is also informative and illustrates further parallels in their structural similarity. In accord with its plane of mirror symmetry that bisects the rhodium centre and boron atoms at the 3 and 8 positions, the ^{11}B NMR spectrum of compound **2** consists of four doublets of rel-

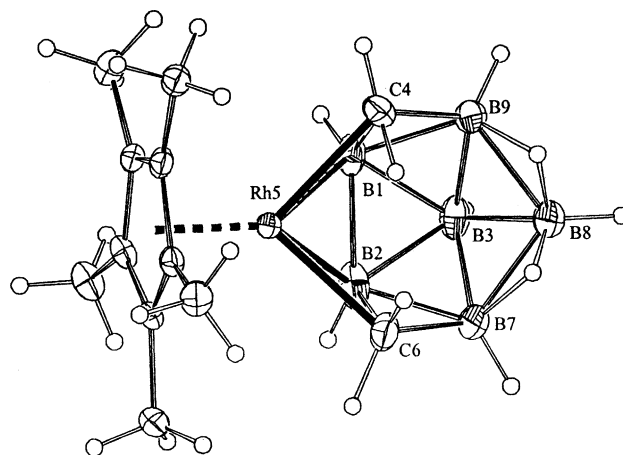


Fig. 1. Illustration of the molecular structure of $(\text{C}_5\text{Me}_5)\text{RhC}_2\text{B}_6\text{H}_{12}$, compound **2**, as determined by single crystal X-ray diffraction. [Selected interatomic distances: average B–B connectivity = 1.807 (10) Å, average B–C connectivity = 1.627 (9) Å, Rh5–B1 = 2.150 (6) Å, Rh5–B2 = 2.142 (8) Å, Rh5–C4 = 2.254 (5) Å, Rh5–C6 = 2.242 (6) Å]. (ellipsoids 30% probability level).

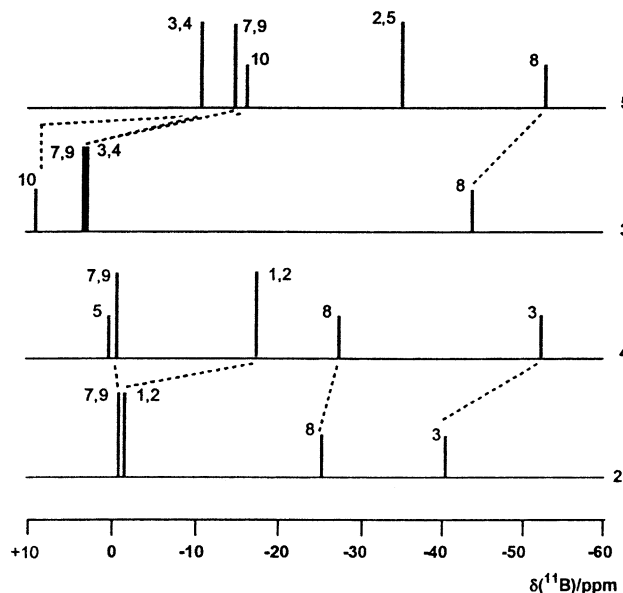
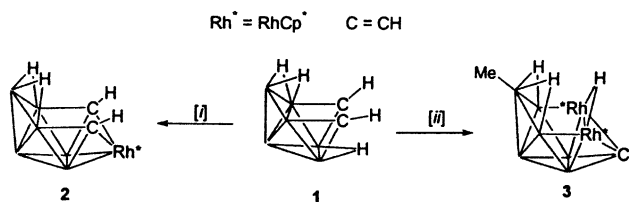


Fig. 2. Stick representation of ^{11}B chemical shifts and relative intensities for compounds $\text{Cp}^*\text{RhC}_2\text{B}_6\text{H}_{12}$ (**2**), $4,6\text{-C}_2\text{B}_7\text{H}_{13}$ (**4**, data from [5]), $\text{Cp}_2^*\text{Rh}_2\text{CB}_6\text{H}_9(\text{CH}_3)$ (**3**), and $1\text{-CB}_8\text{H}_{12}$ (**5**, data from [7]).



Scheme 2. Simplified scheme for the formation of $[5\text{-Cp}^*\text{-}arachno\text{-}5,4,6\text{-RhC}_2\text{B}_6\text{H}_{12}]$ (**2**) and $[2, 5\text{-Cp}_2^*\text{-}10\text{-Me-nido-}2, 5, 1\text{-Rh}_2\text{CB}_6\text{H}_9]$ (**3**) from anion **1**.

ative intensities 2:2:1:1. These resonances are readily assigned to molecular boron atom positions by ^{11}B – ^{11}B COSY NMR spectroscopy and by comparison with the already assigned ^{11}B spectrum of carborane **4** [5]. The two spectra are very similar apart from the obvious absence of the B(5) signal in the spectrum of compound **2** where the rhodium metal atom is situated, and the downfield shift in the spectrum of **2** of the resonances for the boron atoms B(1), B(2) and B(3) of about 15 ppm, which may be accounted for by the fact that

it is these boron atoms that are adjacent to and, thus, subject to the influence of the rhodium centre.

Of interest is the fine-coupling observed in the ^1H resonances for the (*exo*-CH) and (*endo*-CH) proton nuclei in compound **2**. In both cases a well resolved quartet coupling pattern may be seen, which is due to $^3J(^1\text{H}-^1\text{H})$ coupling of approximately 8 Hz between the carbon-bound hydrogen atoms and hydrogen nuclei bound to adjacent boron vertices. This phenomenon is not seen so clearly in the ^1H spectrum of **4**, which was measured using the same instrument, with the same solvent and on the same day.

The reaction chemistry of compound **4** is rich [6], which gave us reason to anticipate that compound **2** may have a similar variety in its reactivity. In this context, we are currently looking into ways of increasing the yield in which it is synthesized. We have come to believe that the reactivity of the helmet anion is, to an extent, dependent on the nature of the counter cation. We are, therefore, currently investigating the synthesis of compound **2** from different salts of *hypho*-[$\text{C}_2\text{B}_6\text{H}_{13}$] $^-$.

The single-crystal X-ray diffraction and NMR spectroscopic results for compound **2** both confirm the presence of four cluster open-face hydrogen atoms: two B–H μ –B bridging hydrogen atoms and two C–H $_{\text{endo}}$ hydrogen atoms. These atoms can theoretically be replaced by a second rhodium vertex. In this context, the reaction that generated compound **2** was repeated, but with the use of a two-molar excess of $[\text{Cp}^*\text{RhCl}_2]_2$ and in the presence of proton sponge (path [ii] of Scheme 2). After overnight reaction at room temperature a small sample of the reaction mixture was taken and subjected to TLC, which showed the consumption of anion **1** and the presence of several coloured components. Separation of this mixture has resulted in the isolation and characterization of the major product as $[2, 5\text{-Cp}_2^*-10\text{-Me-}n\text{-ido-}2, 5, 1\text{-Rh}_2\text{CB}_8\text{H}_9]$ (compound **3**). Fig. 3 is an ORTEP representation of the crystallographically determined structure of compound **3**, which displays the same nine-vertex *nido* molecular geometry as the previously reported *nido*-1-CB $_8\text{H}_{12}$ monocarbaborane (compound **5**, for new numbering see Scheme 3) [7]. As far as we are aware, this geometry has not previously been observed in metallacarborane chemistry.

Although the starting-material $\{\text{C}_2\text{B}_6\}$ skeleton of anion **1** remains traceable in the structure of compound **2** – the addition of the rhodium centre only replacing one open-face bridging hydrogen atom – in compound **3** the original $\{\text{C}_2\text{B}_6\}$ skeleton is missing completely (see Scheme 2). Instead one carbon atom has been expelled from the polyhedral framework and is moved to an *exo*-ligand site, and the remaining cluster atoms have undergone a rearrangement of positions such that the two rhodium atoms in **3** now occupy the positions of the two carbon atoms in **2**, and the single carbon atom in **3** now occupies the position of the single rhodium at-

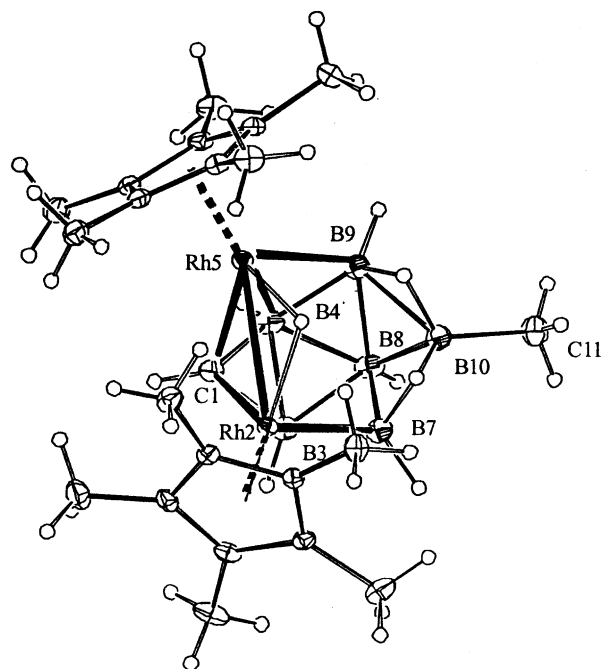
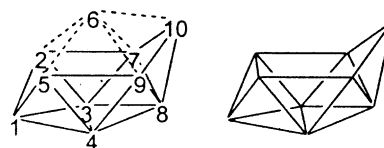


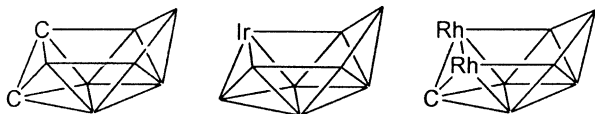
Fig. 3. View on the A molecule of compound **3**. Selected interatomic distances: average B–B connectivity=1.800 (4) Å, average B–C connectivity=1.615 (4) Å, Rh2–Rh5 2.8510(3) Å, Rh2–C1=2.047 (3) Å, Rh2–B3=2.195 (3) Å, Rh2–B7=2.232 (3) Å, Rh5–C1=2.052 (3) Å, Rh5–B4 2.202(3) Å, Rh5–B9 2.215(3) Å. (ellipsoids 30% probability level).



Scheme 3. Derivation of a nine-vertex *nido* polyhedron by the removal of one vertex from a ten-vertex *closo* polyhedron.

om in **2**. This results in compound **3** having a *nido* geometry exactly the same as proposed earlier for monocarbaborane **5** [7]. This similarity is further demonstrated by graphical comparison of the ^{11}B NMR spectra of compound **3** and carborane **5** shown in Fig. 2 (upper traces). The figure demonstrates that the spectra of the Rh species **3** are generally shifted downfield, especially the resonances of boron vertices adjacent to the Rh atoms. Parallels in structural similarity between **3** and **5** are thus clearly shown.

This *nido* geometry is also seen in the carborane, $\text{C}_2\text{B}_7\text{H}_9\text{Me}_2$ [8], and in a single metallaborane example; $(\text{CO})(\text{PMe}_3)_2\text{IrB}_8\text{H}_{11}$ [9]. Scheme 4 shows the polyhedral skeletons of these two examples and also that of compound **3**. The single cage-carbon atom is situated, as might be expected, in the 1 position of lowest connectivity. The two rhodium atoms occupy the 2 and 5 positions in the nine-vertex skeleton of **3** and if compared to $(\text{CO})(\text{PMe}_3)_2\text{IrB}_8\text{H}_{11}$ one rhodium atom is located in



Scheme 4. The polyhedral skeletons of $1,2\text{-C}_2\text{B}_7\text{H}_9\text{Me}_2$, $(\text{CO})(\text{PMe}_3)_2\text{IrB}_8\text{H}_{11}$ and compound **3**.

an analogous position as the $\{(\text{CO})(\text{PM}(\text{e}_3)_2\text{Ir})\}$ fragment in $(\text{CO})(\text{PMe}_3)_2\text{IrB}_8\text{H}_{11}$ and the second in an adjacent position, replacing a $\{\text{BH}\}$ vertex. In this context, each rhodium fragment in compound **3** may be thought of as *isoelectronic* to a $\{\text{BH}\}$ unit and, in this manner, contributes two electrons to the overall cluster-bonding scheme.

Compound **3** is air-stable over long periods: of time and may be heated up to high temperatures without decomposition or change. This makes it quite different from compound **2**, which slowly decomposes at room temperature and rapidly at elevated temperatures. Measured ^{11}B NMR parameters of compound **3** reflect its crystallographic symmetry, giving the expected 2:2:1:1 intensity patterns, however, with the two intensity 2 peaks overlapping.

The hydrogen atom that bridges the two rhodium atoms in compound **3** is clearly identifiable in the proton spectrum as a triplet of splitting $^1J(^1\text{H}\text{--}^{103}\text{Rh}) = 30.4$ Hz. Its chemical shift is in a position (-22.95 ppm) that is unusually high for boron-containing cluster compounds, and is perhaps one of the highest ^1H resonance positions recorded for metallacarborane species. As far as the authors know, no other example of a bridging hydrogen atom between two rhodium centres has been reported. In a geometrical context, the positions of the three bridging hydrogens in **3** are identical with those found in *nido*-1- CB_8H_{12} [7] with the other two equivalent B–H–B bridging hydrogens resonating at -1.0 ppm.

3. Conclusion

Under the conditions described above both one rhodium vertex and two rhodium vertices have been inserted into the $[\text{C}_2\text{B}_6\text{H}_{13}]^-$ framework in **1**, with the latter causing an interesting alteration in the carborane framework of the starting anion involving the expulsion of one carbon cluster vertex as a methyl *exo*-substituent group, and the generation of a nine-vertex *nido* polyhedral geometry. The propensity for this reactivity (metal fragment insertion occurring at room temperature), suggests that further chemistry surrounding the *hypho* anion **1** will be rich in content. The relative ease in which anion **1** is made and its reactivity observed herein surmounts to a large potential.

Further work in the study of the reactivity of anion **1** is currently under-way and further experimental findings are set to be submitted for refereeing soon.

4. Experimental

4.1. General

Reactions were carried out in dry solvents (tetrahydrofuran, hexane, and dichloromethane) under dry nitrogen, but subsequent manipulatory and separatory procedures were carried out in air. Preparative thin-layer chromatography (TLC) was carried out using 1 mm layers of silica gel G (Fluka, type GF254) made from water slurries on glass plates of dimensions 20×20 cm², followed by drying in air at 80°C .; components were located visually. NMR spectroscopy was performed at 9.4 T in CD_3CN on a Varian MERCURY 400 High Resolution System. Chemical shifts δ are given in ppm relative to $\Xi = 100$ MHz for $\delta(^1\text{H})$ (± 0.05 ppm) (nominally TMS) and $\Xi = 32.083972$ MHz for $\delta(^{11}\text{B})$ (± 0.5 ppm) (nominally Et_2OBF_3 in CDCl_3) [10]. Ξ is as defined by McFarlane [11].

4.1.1. Isolation of $(\text{C}_5\text{Me}_5)\text{RhC}_2\text{B}_6\text{H}_{12}$ (compound **2**) from the reaction of $[\text{C}_2\text{B}_6\text{H}_{13}][\text{NMe}_4]$ with $[\text{RhCp}^*\text{Cl}_2]_2$

To a dry THF solution of $[\text{C}_2\text{B}_6\text{H}_{13}][\text{NMe}_4]$ (0.25 g; 1.4 mmol) was added a molar equivalent of $[\text{RhCp}^*\text{Cl}_2]_2$ (0.88 g; 1.4 mmol). This mixture was left to stir at room temperature and under a stream of Argon for a period of approximately 8 h. During this period small aliquots of the reaction mixture were taken and TLC measurements performed in order to monitor the progress of reaction [silica G on Al foil {Silufol (Kavalier, Prague)}, with components being detected by iodine vapour, followed by aqueous AgNO_3 spray]. Once all of the starting compound **1** was consumed the THF solvent was evaporated in vacuo (room temperature and water pump), and the resinous residue extracted with dichloromethane (2×20 ml) and filtered through a small amount of silica. The filtrate was subjected to column chromatography (2×25 cm, silica gel, 70–220 mesh) using a mixture of hexane–dichloromethane (1:1) as mobile phase. The major component of this chromatography was an orange band (R_f 0.6), which was collected and hence further purified on plate TLC and found to be $(\text{C}_5\text{Me}_5)\text{RhC}_2\text{B}_6\text{H}_{12}$ (**2**) (0.1 g, 0.31 mmol, 22%). Red crystals suitable for single-crystal X-ray diffraction were grown by slow evaporation of a diethylether solution of compound **2**. For **2**: m.p. 167°C , ^{11}B NMR (128.3 MHz, 25°C): $\delta = -0.7$ (d, 2B, B7,9), -1.4 (d, $^1J(\text{B},\text{H}) = \sim 145$ Hz, 2B, B1,2), -25.4 (d, $^1J(\text{B},\text{H}) = 174$ Hz, 1B, B8), -40.7 (d, d, $^1J(\text{B},\text{H}) = 137$ Hz, 1B, B3), all theoretical $[^{11}\text{B}\text{--}^{11}\text{B}]$ -COSY crosspeaks observed, except for B7,9–B8 and B1,2–B8; $^1\text{H}\{^{11}\text{B}\}$ NMR (400 MHz, 25°C): $\delta = 3.03$ (s, 2H, H7,9), 2.17 (s, 2H, H1,2), 1.95 (s, 1H, H8), 0.13 (s, 1H, H3), -0.38 (m, $^3J(\text{H},\text{H}) = \sim 8$ Hz, 1H, *exo*-H4, 6), -1.86 (m, $^1J(\text{H},\text{H}) = \sim 8$ Hz, 1H, *endo*-H4, 6), -2.33 (s, 2H, $\mu\text{H}7,8\text{--}8,9$).

4.1.2. Isolation of $(C_5Me_5)_2Rh_2CB_6H_9(CH_3)$ (compound 3) from the reaction of $[C_2B_6H_{13}][NMe_4]$ with $[RhCp^*Cl_2]_2$ and 'proton-sponge'

To a dry THF solution of $[C_2B_6H_{13}][NMe_4]$ (0.25 g; 1.4 mmol) was added a two-molar excess of $[RhCp^*Cl_2]_2$ and (1.76 g; 2.8 mmol) and 1,8-bis-(dimethylamino)-naphthalene (proton-sponge) (0.61 g; 2.8 mmol) and the mixture was allowed to stir at room temperature overnight (10 h). In a similar fashion to the preparation of compound 1, the progress of reaction was monitored by TLC and, once the starting-material had disappeared, the reaction mixture was chromatographed using the same conditions as described above for compound 1. Of the eluted coloured bands observed, the main component, an orange compound of $R_f=0.5$ (1:1 $CH_2Cl_2/n-C_6H_{14}$) was isolated, further purified by plate-TLC chromatography and characterized as $(C_5Me_5)_2Rh_2CB_6H_9(CH_3)$ (compound 3), (0.09 g, 0.17 mmol, 12%). Orange-red crystals suitable for single-crystal X-ray diffraction were grown by slow evaporation of a diethylether solution of compound 3. For 3: m.p. 249 °C, ^{11}B NMR (128.3 MHz, 25 °C): $\delta=9.1$ (d, $^1J(B,H)=\sim 134$ Hz, 1B, B10), 3.6 (d, $^1J(B,H)=\sim 135$ Hz, 4B, 83,4,7,9), -43.0 (d, $^1J(B,H)=\sim 137$ Hz, 1B, B8), all theoretical [$^{11}B-^{11}B$]-COSY crosspeaks observed. $^1H\{^{11}B\}$ NMR (400 MHz, 25 °C): $\delta=3.61$ (s, 1H, H1), 2.25 (s, 2H, H7,9), 2.07 (s, 2H, H3,4), -0.81 (s, 1H, H8), -1.00 (s, 2H, $\mu H7,10-9,10$), -22.95 (t, $^1J(Rh-H)=30.4$ Hz, $\mu H2,5$).

4.2. X-ray crystallography

4.2.1. Crystal data for $(C_5Me_5)RhC_2B_6H_{12}$, 2

$RhC_{12}B_6H_{27}$: $M=339.11$, orthorhombic, $a=10.9970$ (3), $b=11.3400$ (3), $c=12.6690$ (4) Å, $U=1579.90$ (8) Å³, $X=0.71073$ Å, $T=150(2)$ K, space group $P2_12_12_1$, $Z=4$, $\mu(Mo K\alpha)=1.059$ mm⁻¹, $R_{int}=0.0712$ for 26,845 reflections and $wR(F^2)=0.0783$ for all 3458 unique reflections.

4.2.2. Crystal data for $(C_5Me_5)_2Rh_2CB_6H_9(CH_3)$, 3

$Rh_2C_{22}B_6H_{42}$: $M=577.24$, monoclinic, $a=14.37200$ (10), $b=19.9670$ (2), $c=18.0630$ (2) Å, $U=5159.33$ (8) Å³, $\lambda=0.71073$ Å, $T=150(2)$ K, space group $P2_1/n$, $Z=8$, $\mu(Mo K\alpha)=1.287$ mm⁻¹, $R_{int}=0.0557$ for 82,141 reflections and $wR(F^2)=0.0657$ for all 11,826 unique reflections.

5. Supplementary material

Crystallographic data for the structural analysis has been deposited with the Cambridge Crystallographic

Data Centre, CCDC Nos. 223150 and 223151 for the compounds 2 and 3.

Acknowledgement

We thank the Ministry of Education of the Czech Republic (project no. LNOOA028) for support. We also offer a special thanks to Prof. Illnerová and to the British Council for their kind financial support to M. Londesborough.

References

- [1] T. Jelinek, J. Plešek, S. Heřmánek, B. Štíbr, Main Group Met. Chem. 10 (1987) 401.
- [2] T. Jelinek, J. Holub, B. Štíbr, X.L.R. Fontaine, J.D. Kennedy, Collect. Czech. Chem. Commun. 59 (1994) 1584–1595.
- [3] See for example; R.N. Macias, S.A. Barret, J. Bould, U. Dorfler, J. Holub, J.D. Kennedy, M. Thornton-Pett, B. Štíbr, Acta Cryst. C 57 (2001) 520–522; M. Bown, B. Gruner, B. Štíbr, X.L.R. Fontaine, M. Thornton-Pett, J.D. Kennedy, J. Organomet. Chem. 614 (2000) 269–282; U. Dorfler, W. Glegg, M. Thornton-Pett, J.D. Kennedy, J. Chem. Soc., Dalton Trans. 14 (1998) 2353–2358; P. Kair, J.D. Kennedy, M. Thornton-Pett, T. Jelinek, B. Štíbr, J. Chem. Soc., Dalton Trans. 12 (1997) 2005–2007; U. Dorfler, J.D. Kennedy, L. Barton, C.M. Collins, W.P. Rath, J. Chem. Soc., Dalton Trans. 5 (1997) 707–708.
- [4] J. Bould, R. Greatrex, J.D. Kennedy, D.L. Ormsby, M.G.S. Londesborough, K.L.F. Callaghan, M. Thornton-Pett, T.R. Spalding, S.J. Teat, W. Clegg, H. Fang, N.P. Rath, L. Barton, J. Am. Chem. Soc. 124 (2002) 7429–7439.
- [5] P.M. Garret, T.A. George, M.F. Hawthorne, Inorg. Chem. 8 (1969) 2008; B. Štíbr, J. Plešek, S. Heřmánek, Collect. Czech. Chem. Commun. 38 (1973) 338.
- [6] See for example; L. Mikulašek, B. Gruner, I. Čisařová, B. Štíbr, J. Chem. Soc., Dalton Trans. 7 (2003) 1332–1336; J.H. Jones, J.D. Kennedy, B. Štíbr, Inorg. Chim. Acta 218 (1994) 1–3; T. Jelinek, J. Plešek, S. Heřmánek, B. Štíbr, Polyhedron 7 (1986) 1303–1305.
- [7] K. Baše, B. Štíbr, J. Dolanský, J. Duben, Collect. Czech. Chem. Commun. 46 (1981) 2345–2353; S. Heřmánek, J. Fusek, B. Štíbr, J. Plešek, T. Jelinek, Polyhedron 5 (1986) 1873.
- [8] J.C. Huffman, W.E. Streib, J. Chem. Soc., Chem. Commun. 582 (1972) 665–666.
- [9] J. Bould, N.N. Greenwood, J.D. Kennedy, J. Chem. Soc., Dalton Trans. (1984) 2477–2485; J. Bould, J.D. Kennedy, L. Barton, N.P. Rath, Chem. Commun. 24 (1997) 2405–2406.
- [10] See, for example J.D. Kennedy, in: J. Mason (Ed.), Boron, Multinuclear NMR, Plenum, New York and London, 1987, pp. 221–254 and references therein (Chapter 8).
- [11] W. McFarlane, Proc. R. Soc. (Lond.), Series A 306 (1968) 185.